CYCLIC CHANGES IN SOLAR ROTATION INFERRED FROM TEMPORAL CHANGES IN THE MEAN MAGNETIC FIELD

A. V. MORDVINOV and L. A. PLYUSNINA
Institute of Solar-Terrestrial Physics, P.O. Box 4026, Irkutsk 33, 664033, Russia
(E-mail: avm@iszf.irk.ru)

(Received 23 March 2000; accepted 24 July 2000)

Abstract. Time–frequency variability of the solar mean magnetic field (SMMF) was studied, based on a continuous wavelet analysis. The rotational modulation of the SMMF dominates the wavelet spectrum at 27–30 and 13.5-day time scales. The rotational variation, in turn, is amplitude-modulated by the quasi-biennial periodicity in the SMMF. This is caused by magnetic field eruptions. Rigidly rotating modes appear in the time–longitude distribution of the large-scale magnetic field that is plotted from a deconvolution of the SMMF time series with a Carrington period. These rotational modes coexist and transform into one another over an 11-yr cycle. The modes with periods of 27.8–28.0 days dominate the phase of activity rise, whereas the 27-day rotational mode dominates the declining phase of the 11-yr cycle. The rotational modes with periods of 29–30 days occurred episodically. Most of the features in the time–longitude distribution of the SMMF are identifiable with those in similar diagrams of the solar background magnetic fields. They represent a combined effect of the background magnetic fields from both hemispheres. Eruptions of magnetic fields lead to dramatic changes in the picture of solar rotation and correlate well with the polarity asymmetry in the SMMF signal. The polarity asymmetry in the SMMF time series exhibits both long-term changes and a 22-yr cyclic behaviour, depending on the reversals of the global magnetic field in cycles 20–23.

1. Introduction

The solar mean magnetic field (SMMF) is a fundamental physical parameter that quantifies the magnetic field of the Sun as a star and governs the space weather in the solar system. The SMMF signal results from the convolution of the magnetic field distribution across the solar disk with the weighting function of a magnetograph (Scherrer *et al.*, 1977; Kotov and Severny, 1983). The SMMF varies over a wide range of time scales due to the mechanisms of eruptions, transport and diffusion of the solar magnetic fields (Sheeley, De Vore, and Shampine, 1986). Apparent changes in the SMMF are caused by rotational modulation and are due to the Earth's excursions relative to the solar equatorial plane in the course of its orbital motion (Ponyavin, 1998). Temporal changes in the SMMF and their power spectra have been scrutinized in previous studies based on measurements from the Crimean, Stanford, and Sayan observatories (Kotov and Severny, 1983; Scherrer *et al.*, 1977; Grigoryev and Demidov, 1987). In this paper the time–frequency

Solar Physics **197:** 1–9, 2000.

variability of the SMMF is studied using wavelet analysis that is appropriate for analyzing nonsteady time series (Chui, 1992).

Despite recent advances in helioseismology, the picture of external manifestations of solar rotation that is derived from different tracers is complicated and is sometimes contradictory; moreover, it depends on the level of magnetic activity (Stenflo, 1989; Ananyev and Obridko, 1999). Discrete modes of rigid rotation (Erofeev, 1996; Plyusnina, 1999) and the torsional oscillations (Howard and LaBonte, 1987) are observed against the background of the differential rotation of the Sun. When derived from temporal changes in the SMMF, solar rotation shows the net effect of the solar magnetic field which results mainly from the background magnetic fields (Kotov, Stepanyan, and Scherbakova, 1977).

2. Wavelet Analysis of the SMMF

A continuous wavelet analysis was applied to a composite time series of the SMMF for 1968–2000. A Stanford data set of the SMMF was complemented by earlier measurements obtained at the Crimean observatory during 1968–1975. During the overlapping period 1975–1976, composite values of the SMMF were averaged with weights estimated by Haneychuk (1998). The composite SMMF time series and the modulus of Morlet wavelet transform are shown in Figure 1. The wavelet spectrum clearly shows a time-frequency behaviour of the SMMF over a wide range of time scales.

According to the uncertainty principle, the resolution of the analysis in the time-period space is restricted to the range $2\delta_t \times 2\delta_P$. At the worst, the uncertainties in time and period are $\delta_t \approx 8$ d, $\delta_P \approx 7$ d at the Carrington period P_C. Because of the limited resolution on the timescales around the period of solar rotation, we see no set of discrete rotational modes, which appear in the power spectra (Kotov, 1987). The periodicity around 13.5 days appears episodically. It is caused by the four-sector structure of the large scale magnetic field and appears also as a harmonic of rotational modulation. The 9-day periodicity of the SMMF, and many of the solar indices seem to originate from the convolution of spatial inhomogeneities of the magnetic field with the limb darkening function (Mordvinov, 1995).

The horizontal cross-section of the wavelet spectrum at the timescale of the rotational period shows prominent patterns which recur at about 1.5–2 yr time intervals, which appear as an amplitude modulation of the rotational periodicity. There are four and five such patterns in cycles 21 and 22, respectively. They result from eruptions of magnetic fields, which appear with quasi-biennial periodicity (Erofeev, 1996). As a new portion of magnetic field emerges, the amplitude of 27-day variation of the SMMF increases.

Long-term changes in the SMMF appear over a timescale range of about 1–2 years. The amplitude of quasi-biennial oscillations vanishes at epochs of activity minima and peaks in 1980–1982, and in 1991–1992. Hence, we can conclude

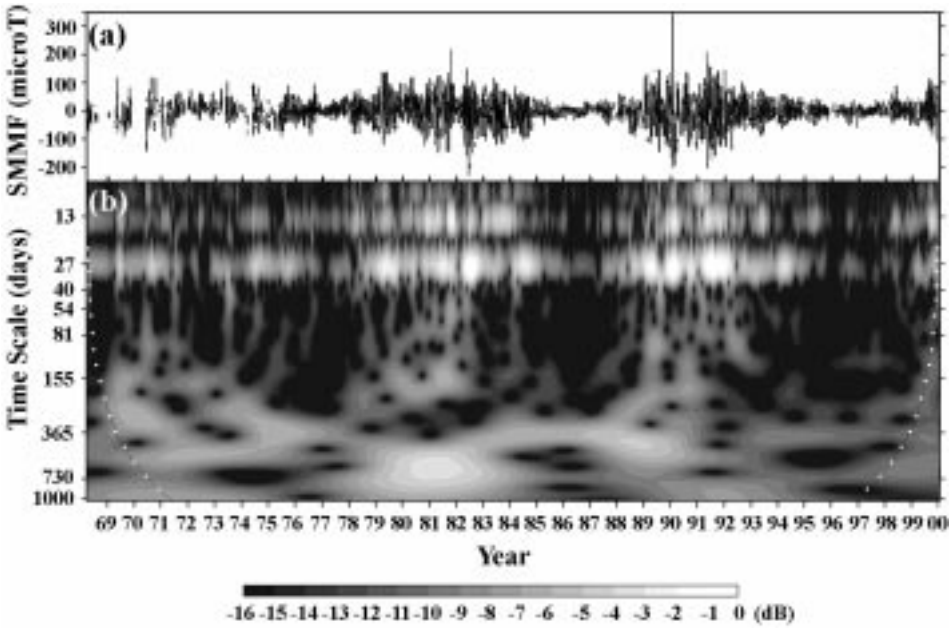

Figure 1. The composite SMMF time series (a), and Morlet wavelet modulus normalized to its maximum value (b). The maximum of the spectrum corresponds to 0 decibel, and this is shown in white. The dotted lines indicate the edge distortions of the spectrum.

that quasi-biennial oscillations in the SMMF are related to the level of magnetic activity. By contrast, the annual periodicity in the SMMF is well defined during epochs of minima. The annual modulation originates from the variable contribution of the solar magnetic dipole to the SMMF signal. As the Earth travels between the extreme points relative to the solar equator in the course of its orbital motion, the contribution of the global magnetic dipole varies. There are weak intermediate-term variations at about a 155-day time scale in the wavelet spectrum. The spectral power increases there during the maxima of solar activity in 1980–1982, and in 1989–1991, and appears immediately behind the first peaks at the rotational timescale. Wavelet spectra of magnetic and thermodynamic parameters of the Sun display similar patterns at the intermediate timescales. They seem to result from a relaxation of thermomagnetic perturbations over a solar cycle (Willson and Mordvinov, 1999).

3. Spatio-Temporal Analysis of the SMMF

The time–longitude distribution of the SMMF in the Bartels format roughly characterizes the structure of the large scale magnetic field and the solar rotation. Nevertheless, these diagrams do not trace the solar rotation in detail because of a systematic shift accumulated over a long time interval. In this paper we have stud-

ied the time–longitude distribution of the magnetic field, plotted from the deconvolution of the SMMF time series with the Carrington period $P_C = 27.2753$ days. Such diagrams are sensitive to effects of rigidly rotating modes. These modes with periods larger or smaller than P_C arrange the magnetic fields into oppositely inclined structures on the diagrams. To construct a time–longitude distribution we rearranged the time series of the SMMF into subsets according to the Carrington rotations and plotted these subsets as the longitude scans line-by-line on a gray scale. While the SMMF signal results from a convolution of the magnetic field distribution over the solar disk with the weighting function of a magnetograph, the derivation of a spatial distribution of the magnetic field from temporal changes in the SMMF is an inverse operation or a deconvolution of the SMMF time series.

A composite SMMF time series and its time–longitude diagram in the Carrington format are shown in Figures 2(b) and 2(a), respectively. The corresponding gray scale for Figure 2(a) is shown at the top. It is of little importance whether larger or smaller SMMF values trace the solar rotation. Therefore, we normalized the values of the SMMF within each Carrington rotation to a maximum value for this rotation. This normalization reveals rotational patterns in a compatible form regardless of the level of magnetic activity. Figure 2(c) shows a time–longitude distribution of the normalized SMMF that is denoised with 2D wavelet decomposition. The positive polarity is shown in bright halftones against the 50%-gray background, whereas the negative polarity is shown in dark halftones. In Figure 2(c), bright and dark patterns are arranged as inclined structures, which reveal discrete rigidly rotating modes. The positive polarity displays well-defined bright patterns in cycle 21, which are clearly related to cyclic behaviour of solar activity. The mode with a period of 27.8 days is dominant for 1977–1981 at the phase of increasing activity. The regime of solar rotation changed immediately after the activity maximum. The mode with a period of 26.8 days persisted from 1982 during the phase of decreasing activity. The rotational mode with a period of 28.4 days appeared episodically. By the year of minimum activity, in 1986, the rotational mode with a period of ($P = 26.8$ d) is terminated. In cycle 22, during the phase of rising activity, one can see the rotational modes with 28.0-, 28.3-, and 30.0-day periods in the positive polarity. Rotational modes with periods of 26.8 and 27.0 days are dominant during the phase of decreasing activity. The overall picture of rotation looks much more complicated as compared to that for cycle 21. In cycle 20, the picture of time–longitude distribution looks fuzzy because of earlier noisy measurements. Nevertheless, we can see the rotational mode with a period of 27.0 days, which dominates the declining phase during 1970–1977. The occurrences of the 27-day rotational mode are in good agreement with results obtained by Erofeev (1996). The rotational mode with a period about of 28 d persisted during 1972–1973 as a weak inclined and fragmentary pattern. At the beginning of cycle 23, there are subtle patterns which correspond to the rigidly rotating modes with 28–29 day periods against the noisy background. In cycles 20–23, the negative polarity

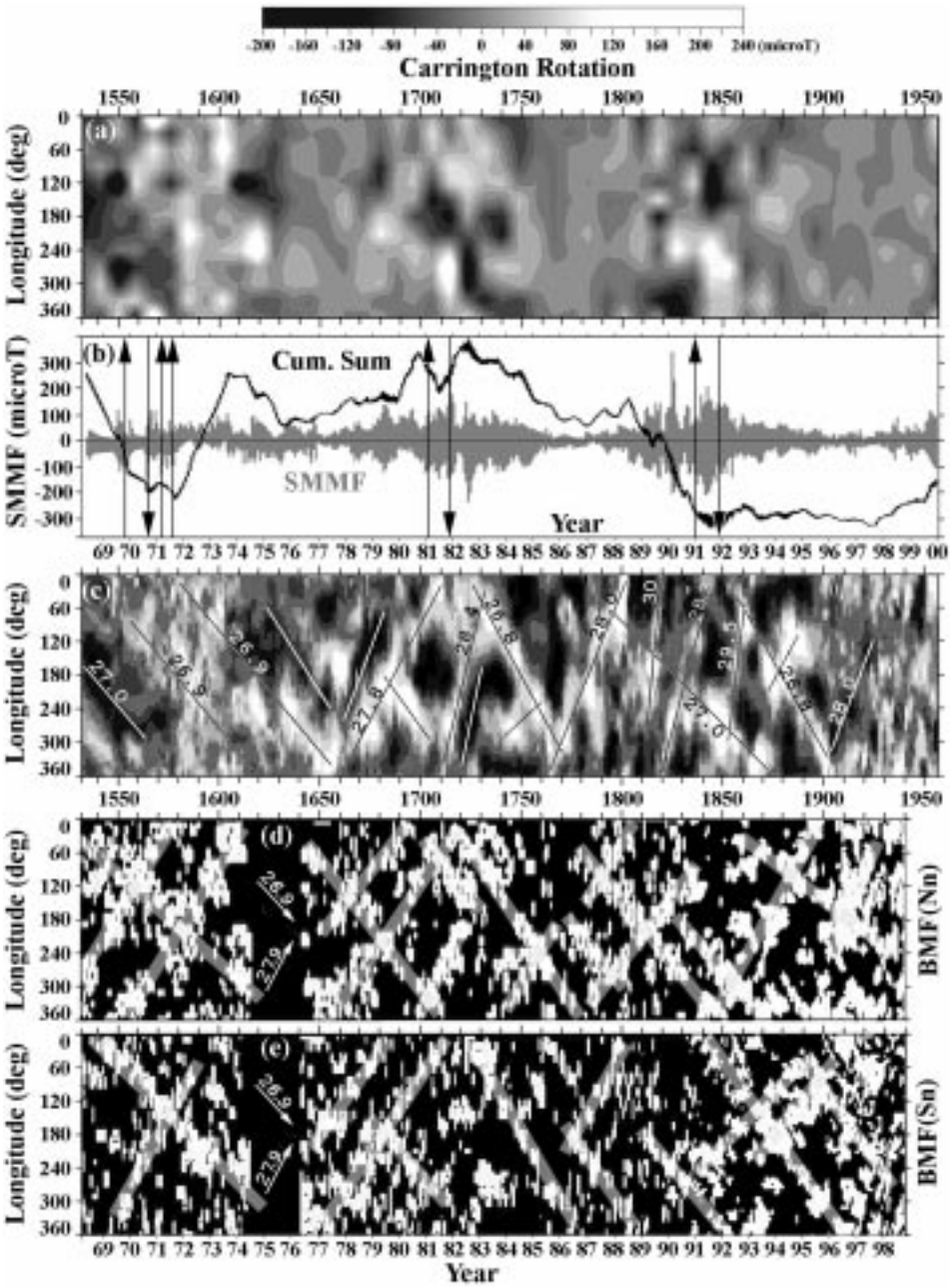

Figure 2. Time–longitude distribution of SMMF (a), the composite SMMF, its cumulative sum (b), and time–longitude diagram of normalized SMMF (c) are juxtaposed with BMF stack plots for positive polarity both in the north (d), and south (e) hemispheres of the Sun.

behaves somewhat independently, and sometimes displays parallel patterns shown in dark.

Thus, the picture of solar rotation varies over an 11-yr cycle and from cycle to cycle. As a rule, rotational modes with a period of 27.8–30 days dominate the phase of rising activity, whereas the mode with period of 27 days dominates the phase of decreasing activity. To identify the particular contributions of the positive and negative polarities separately in both hemispheres, a time–longitude analysis of the background magnetic field (BMF) was carried out.

4. A Comparative Analysis of the SMMF and BMF in the Time–Longitude Space

To plot the time–longitude diagram of the BMF we use a robust technique (Plyusnina, 1999) which is described below. The method characterizes the BMF using Hα or synoptic maps of magnetic field binned in cells $10^\circ \times 10^\circ$ within the latitude zones $0, +40^\circ$ and $0, -40^\circ$. From the synoptic maps we construct a quantitative characteristic of the BMF according to the following procedure. We examine all the cells and estimate their dominant polarity. If the positive or negative polarity covers more than 60% of the cell area, the magnetic field in this cell is quantified as $+1$ or -1, respectively. If there is no dominant polarity in the cell, this is quantified by zero. We obtain a longitudinal distrubution of the BMF, by summarizing all estimated values over the latitude within each longitude interval and separately for each hemisphere. In these summarized distribution we then keep the values ± 3, 4 and reject the values ± 1, 2 by setting them to zero. In doing so, we obtain a robust characteristic of the BMF distribution, thereby excluding the influence of small scale active regions.

Figures 2(d) and 2(e) show time–longitude stack plots of the BMF denoised with 2D wavelet decomposition for positive polarity in the vicinity of the solar equator for the northern and southern hemispheres, respectively. The bright features are arranged again as inclined patterns. These inclined patterns which correspond to the rotational modes with periods of 27 and 28–29 days dominate the time–longitude diagrams of both the BMF and the SMMF. We highlighted these patterns in Figures 2(d) and 2(e). We can identify most of the prominent features in the time–longitude diagram of the normalized SMMF with similar patterns in the BMF diagrams, especially if they appear in both hemispheres simultaneously. There are also some features in the time–longitude diagram of the SMMF resulting from only one hemisphere. However, the degree of correspondence between the BMF and the SMMF varies from cycle to cycle. The picture of solar rotation that is derived from the BMF during cycle 20 for the mode of 27 days is in agreement with those derived from the SMMF. Although the modes of the 28–29 days take place on both the SMMF and BMF diagrams, they vary in values of rotation periods. It is possible that this is due to the earlier noisy measurements of the SMMF.

The pictures of solar rotation that are derived from the BMF and SMMF correlate well during cycle 21 and for ascending phase of cycle 22. The degree of agreement between the diagrams is no longer as evident for descending phase of cycle 22 and during the activity rise in cycle 23. The rotational modes of the 28–29-day period appear more clearly in the rotational picture of the BMF, whereas the 27-day mode dominates the rotational picture derived from the SMMF. Nevertheless, even at this period most of the prominent features in the time–longitude diagram of the SMMF have their counterparts in time–longitude diagrams of BMF in one hemisphere or another. It should be noted that at this time interval the magnetic fields have been highly asymmetric about the equator of the Sun (Plyusnina, 1998).

In the wavelet spectrum of the SMMF at the 27-day time scale, power peaks recur with quasi-biennial periodicity. From comparison studies of the wavelet spectrum of the SMMF and time–longitude distributions of magnetic fields we can infer that the occurrence of the rotational modes is usually associated with magnetic field eruptions which occur and recur at a timescale of the rotational period. Thus the magnetic field eruptions modify the rotation of the Sun.

5. Long-Term and Cyclic Changes in the SMMF

Most of the indices of solar activity are additive functions which summarize the activity contributions over the solar disk. To the contrary, the SMMF signal results from the difference of the contributions of opposite magnetic polarities. The sign of the SMMF is governed by the dominant polarity in the magnetic field distribution over the solar disk. To reveal long-term tendencies in the evolution of the large scale magnetic field we estimate the cumulative sum of the SMMF signal as $S(t_i) = \sum_{k=1}^{i} \mathrm{SMMF}(t_k)$. This value roughly characterizes the SMMF integrated over a current time interval. In Figure 2(b), the cumulative sum is juxtaposed with the SMMF. On this plot, the cumulative sum is rescaled according to the formula $S_i^{\mathrm{plot}} = (S_i + 6500)/25$. After the summation, fluctuations in the SMMF compensate each other, and the weak asymmetry of the polarities in the source signal is accumulated in the sum, which exhibits smooth and cyclic changes. The cumulative sum characterizes long-term tendencies in SMMF changes: the dominant magnetic field of positive polarity leads to an increase of the sum, whereas the dominant negative polarity leads to a decrease of the sum. The sensitivity of the cumulative sum is appropriate for describing accurately the asymmetry of the polarities in the SMMF signal. A general behaviour of the magnetic ‘monopole’ from cycle to cycle was studied by Grigoryev and Demidov (1989).

In cycle 21, the curve of cumulative sum has two peaks between the epochs of minimum activity in 1976 and 1986. Magnetic field reversals are marked by the arrows according to Makarov and Makarova (1996). The upward arrows indicate the reversals in the northern hemisphere, and the downward arrows indicate those in

the southern hemishere. In cycle 21, magnetic field reversals cover the time interval 1980.0–1981.8 and occur between two peaks of the cumulative sum. The negative polarity dominates cycle 22 except its beginning, and the character of temporal changes is quite different. The cumulative sum decreased steeply after mid-1988 at the phase of rising activity and at maximum activity. After the reversals of the magnetic field in 1990.8–1991.8, oscillations of the cumulative sum were established, which were decreasing in amplitude until 1998. Since 1998 the cumulative sum has tended to increase. This indicates the predominance of positive polarity during increasing activity in cycle 23. In cycle 20, which is partly covered by the Crimean measurements, we can see again a steep decrease of the cumulative sum, which changed to a steep increase after the period of multiple reversals during 1969–1971.5.

6. Conclusions

Time–longitude diagrams of the SMMF and BMF reveal rigidly rotating modes, which coexist and transform into one another. The regime of rotation of the Sun varies over the 22-yr solar magnetic cycle. The rotational modes with periods of 27.8–28.0 days are dominant in the phase of rising activity, whereas the 27-day rotational mode dominates the phase of decreasing activity. Evolutionary changes of the BMF, and the asymmetry of magnetic polarities are manifested in the picture of solar rotation that is derived from deconvoluted SMMF time series. BMF emerge by portions and lead to changes in the regime of solar rotation.

Changes in the regime of solar rotation correlate well with those in the polarity asymmetry in the SMMF signal. The cumulative sum of SMMF reveals long-term and cyclic changes which are governed by the reversals of the global magnetic field. The dominant polarity in the SMMF signal changed to the opposite polarity after the reversals of the magnetic field. The oscillations of the polarity asymmetry were established after the last reversal in cycle 22 until the beginning of cycle 23.

In the behavior of the polarity asymmetry we can trace the 22-yr Hale magnetic cycle. The annual and quasi-biennial periodicities are superimposed on the long-term changes in the cumulative sum of the SMMF. Every 11-yr cycle demonstrates its peculiarities in the asymmetry behaviour. In cycle 21, changes in the asymmetry display a rise and fall according to the cyclic curve of solar activity. Changes in the asymmetry are balanced in terms of the cumulative sum: by the end of the cycle in 1986 the sum returned to the initial level that occurred in the beginning of the cycle in 1976. The cumulative sum decreased steeply at the ascending phase in cycle 22. Then, after the reversals of the magnetic field, the sum oscillated by the end of cycle 22. The changes in the cumulative sum are not balanced over cycle 22.

It is hard to derive cyclic regularities from the short record of the SMMF. Nevertheless, we can suppose that the solar rotation and polarity asymmetry behave differently for odd and even 11-yr cycles. The parity property suggests some pecu-

liarities of the hydromagnetic dynamo (Pipin, 1999) or reveals an effect of the relic global magnetic field (Benevolenskaya, 1998).

Acknowledgements

The Wilcox Solar Observatory data used in this study were obtained via the web site http://quake.stanford.edu/ wso courtesy of J. T. Hoeksema. The authors thank associates from the Crimean and Stanford observatories for the possibility of processing the SMMF data and BMF synoptic charts. We also thank Drs V. M. Grigoryev, M. L. Demidov, V. V. Pipin and Mr V. G. Mikhalkovsky for useful comments and improving the manuscript. This work was supported by the Russian Foundation for Basic Research through grants 99-02-16088 and 00-15-96659.

References

Ananyev, I. V. and Obridko, V. N.: 1999, *Astron. Zh.* **76**, 942.

Benevolenskaya, E. E.: 1998, *Proc. of Conf. New Cycle of Solar Activity: Observational and Theoretical Aspects*, St. Petersburg, Russia, p. 19.

Chui, C.: 1992, *An Introduction to Wavelets*, Academic Press, New York.

Erofeev, D. V.: 1996, *Solar Phys.* **167**, 25.

Grigoryev, V. M. and Demidov, M. L.: 1987, *Solar Phys.* **114**, 147.

Grigoryev, V. M. and Demidov, M. L.: 1989, in *Proc. Conf. Solar Magnetic Fields and Corona*, Novosibirsk, Russia, p. 108.

Haneychuk, V. I.: 1998, in *Proc. Workshop SOHO6/GONG98*, Boston, June 1–6, p. 797.

Howard, R. and LaBonte, B. J.: 1987, *Astrophys. J.* **239**, L33.

Kotov, V. A.: 1986, *Izv. Krym. Astrofiz. Obs.* **75**, 39.

Kotov, V. A.: 1987, *Izv. Krym. Astrofiz. Obs.* **87**, 90.

Kotov, V. A. and Severny, A. B.: 1983, *Mean Magnetic Field of the Sun as a Star. Catalogue for 1968 –1976*, World Data Center B, Moscow.

Kotov, V. A., Stepanyan, N. N., and Scherbakova, Z. A.: 1977, *Izv. Krym. Astrofiz. Obs.* **56**, 75.

Makarov, V. I. and Makarova, V. V.: 1996, *Solar Phys.* **163**, 267.

Mordvinov, A. V.: 1995, *Astron. Astrophys.* **293**, 572.

Pipin, V. V.: 1999, *Astron. Astrophys.* **346**, 295.

Plyusnina, L. A.: 1998, *Solar Phys.* **180**, 53.

Plyusnina, L. A.: 1999, *Proc. of Conf. Large Scale Structure of Solar Activity*, St. Petersburg, Russia, p. 237.

Ponyavin, D. I.: 1998, *Proc. of Conf. New Cycle of Solar Activity: Observational and Theoretical Aspects*, St. Petersburg, Russia, p. 153.

Scherrer, P. H., Wilcox, J. M., Kotov, V. A., Severny, A. B., and Howard, R.: 1977, *Solar Phys.* **52**, 3.

Sheeley, N. R. Jr., De Vore, C. R., and Shampine, L. R.: 1986, *Solar Phys.* **106**, 251.

Stenflo, J. O.: 1989, *Astron. Astrophys.* **210**, 403.

Willson, R. C. and Mordvinov, A. V.: 1999, *Geophys. Res. Let.* **26**, 3613.